Extracting the CRS parameters: A comparison of two methods.

Denilson Stefanelli*, Lúcio T. Santos and Martin Tygel
State University of Campinas, UNICAMP

Abstract

By stacking on supergathers of sources and receivers of arbitrary location around a central point, the Common-Reflection-Surface (CRS) method is able to produce simulated zero-offset sections of significant signal-to-noise ratio. To do that, the method employs a multi-parameter moveout, the generalized hyperbolic moveout, in which the parameters (three in 2D and eight in 3D) are directly estimated from the multi-coverage data. Among its various advantages, the CRS method has the drawback of a costly estimation of the CRS parameters, presently carried out by multi-parameter semblance analysis applied to the data. Here we compare two different methods to extract the CRS parameters, an automatic local-slope detection (or plane-wave destruction) algorithm, that estimates the parameters at a fraction of the cost, and the conventional CRS method.

Introduction

Introduced by Hubral et al. (1998), the CRS method represents a natural extension of the CMP method on two accounts, namely (a) for each stacking trace location, generally called a central point and usually at a CMP location, it considers a supergather of source-receiver pairs, arbitrarily located with respect to the central point and (b) it uses a multi-parameter stacking moveout, the generalized hyperbolic traveltime, with three parameters in 2D and eight parameters in 3D. For an intuitive, less technical introduction to the CRS method the reader can refer to Hertweck et al. (2007) (see more references therein).

In 2D, the general hyperbolic moveout used in CRS can be written in the form

$$T(x_m,h)^2 = [T_0 + A(x_m - x_0)]^2 + B(x_m - x_0)^2 + Ch^2 \ , \qquad (1)$$

where x_m and h denote, respectively, the midpoint and half-offset coordinates of the source-receiver pair, x_0 is the coordinate of the central point, and T_0 is the traveltime along the ZO central ray. The point where the ZO central ray hits the reflector is called the *normal incidence point (NIP)*. In this way, T_0 is twice the traveltime along the normal ray which connects the NIP to the central point.

In Equation 1, the coefficients, or CRS parameters, A, B and C are given in terms of the conventional CRS parameters (see, e.g., Hubral et al., 1998), β, K_N and K_{NIP}, as

$$A = \frac{2sin\beta}{v_0} \quad B = \frac{2T_0 cos^2\beta}{v_0} K_N \quad C = \frac{2T_0 cos^2\beta}{v_0} K_{NIP} \ , \qquad (2)$$

where v_0 denotes the near-surface medium velocity at the central point, supposed to be known. In Equation 2, β denotes the emergence angle of the ZO ray at the central point, and K_N and K_{NIP} are the wavefront curvatures of the so-called N- and NIP-waves, respectively, also at the central point. As explained in Hubral (1983), the N- and NIP-waves are fictitious *eigenwaves*, namely, they start as wavefronts in the vicinity of central point, hit the reflector, and return to the central point in such a way that the curvatures at the initial and endpoints coincide. The two waves, however, have a different behavior at the point NIP: at that point, (a) the wavefront curvature of the N-wave coincides with the curvature or the reflector and (b) the NIP-wave curvature reduces to a point. Looking at their upward propagating parts, the N-wave behaves as an exploding reflector in the vicinity of the NIP, while the NIP-wave behaves as a point diffraction from the NIP.

Semblance analysis

Conventional estimation of the three CRS parameters is done by coherency analysis using semblance measures (Neidel and Taner, 1971). Since a global three-parameter search is computationally too expensive, that multi-parameter search is broken into three, single-parameter, independent searches (Hubral et al., 1998). The obtained three parameters are taken as initial values for a further local three-parameter search using the full moveout Equation 1. Below, we summarize the three single-parameter searches of the parameters A, B and C.

Search for parameter C

The first search is done on the seismic data organized in common midpoint (CMP) gathers. In this case, setting $x_m = x_0$, Equation 1 becomes

$$T_{CMP}(h)^2 = T(x_0,h)^2 = T_0^2 + Ch^2. \qquad (3)$$

A comparison of Equation 3 and the well-known CMP stack formula reveals that this stage reduces to the classic velocity analysis method, with the difference that it is performed on all time samples, t_0.

After extraction of parameter C, a simulated ZO section can be constructed by CMP stacking. That stacked section is then used for the next stages.

Search for parameter A

Under the assumption of a ZO section, the traveltimes are approximated by setting $h = 0$ in Equation 1. We find,

$$T_{ZO}(x_m)^2 = T(x_m,0)^2 = [T_0 + A(x_m - x_0)]^2 + B(x_m - x_0)^2 \ . \quad (4)$$

In Equation 4, parameters A and B are related to dip and curvature. In order to further reduce the search to one parameter, we set $B = 0$ in Equation 4 to obtain a short-offset approximation

$$T_{ZO}^{\text{plane}}(x_m) = T_0 + A(x_m - x_0) \ . \quad (5)$$

Under Equation 5, the reflection events are locally approximated to plane reflection events. Parameter A is determined by coherency analysis using Equation 5.

Search for parameter B

Setting the previous estimation of parameter A in Equation 4, we can estimate the parameter B using a single-parameter coherence analysis. Following equation 2, the above estimations of A, B and C, provide the corresponding parameters β, K_{NIP} and K_N, under the assumption of a known near-surface velocity, v_0, at the central point.

Estimation from local slopes

Santos et al. (2011) demonstrated that the complete set of CRS parameters can be extracted from seismic data by an application of modern local-slope-extraction. The extraction of local slopes is done by so-called plane-wave destructors and use basically the technique presented in Claerbout (1992), Fomel (2002) and Schleicher et al. (2009). The differential equation that describes a local plane-wave event in a seismic section is given by

$$\psi_y(y,t) + s\psi_t(y,t) = 0 \ , \quad (6)$$

where $\psi(y,t)$ is the wavefield, t is the time coordinate and y is the horizontal coordinate. The local slope is represented by s. For each pair (ξ,τ) in the seismic section, a small window of points (y_i,t_j) is selected. Slope selection is accomplished by the quadratic residual minimization

$$R(s) = \sum_{(i,j)} \left[\Psi_y(y_i,t_j) + s\frac{\Delta y}{\Delta t}\Psi_t(y_i,t_j) \right]^2 \ , \quad (7)$$

where $\Psi_y(y_i,t_j)/\Delta y$ and $\Psi_t(y_i,t_j)/\Delta t$ are discretized values for the derivatives, ψ_y and ψ_t. The solution is given by

$$s^*(\xi,\tau) = -\frac{\Delta t}{\Delta y}\frac{\sum_{(i,j)}\Psi_y(y_i,t_j)\Psi_t(y_i,t_j)}{\sum_{(i,j)}\Psi_t^2(y_i,t_j)} \ , \quad (8)$$

where (ξ,τ) is the center of selected window.

As shown in Santos et al. (2011), an estimation of parameters A, B and C can be obtained if local slopes of common-midpoint (CMP) and common-offset (CO) gathers are estimated. A summary of the procedure is described below

CMP gathers: Under the usual assumption of horizontally stratified (or small-dip) media, the ray parameter for the reflection ray in the CMP gather with fixed central point (midpoint) x_0, can be approximated by the traveltime slope (Castagna and Backus, 1993). The derivative of Equation 3 with respect to source-receiver offset $2h$ yelds

$$p = \frac{1}{2}\frac{d}{dh}T_{CMP} = \frac{Ch}{2T_{CMP}}. \quad (9)$$

Thus, if we know the local slope $p = p(h,t)$ in a CMP gather, we can use Equations 9 and 3 to eliminate C from the moveout equation 3. This provides us with the NMO coordinate map (Ottolini, 1983)

$$t_0 = \sqrt{t^2 - 2ht\,p(h,t)} \ , \quad (10)$$

wich describes the relationship between the coordinates (h,t) in a CMP section and the corresponding ZO time t_0 at x_0. Rewriting Equation 9, we see that an estimate of parameter C at half-offset h and time t is given by

$$c(h,t) = \frac{2t\,p(h,t)}{h} \ . \quad (11)$$

Using Equation 10 we can transfer the obtained value of c to the C-parameter section at (x_0,t_0). Since there are redundant information from all available half-offsets, the final $C(x_0,t_0)$ can be calculated by averaging over all $c(h,t)$ that correspond to the same (x_0,t_0). In our numerical examples, this averaging uses the coherence measure associated with the extracted p at (h,t) as a weigth function.

CO gathers: The CRS parameters A and B can be determined from a CO gather in the vicinity of x_0. For the case of a CO gather with a fixed half-offset $h = h_0$, Equation 1 reduces to

$$T_{CO}(x_m) = T(x_m,h_0) = \sqrt{T_{CMP}(h_0)^2 + 2AT_0(x_m - x_0) + D(x_m - x_0)^2}, \quad (12)$$

where the new parameter D is given by

$$D = A^2 + B \ , \quad (13)$$

and T_{CMP} is the traveltime for the offset ray with midpoint at x_0 given in terms of the ZO traveltime T_0 by Equation 3 with $h = h_0$.

From Equation 12, the local slopes $q(x_m, t = T_{CO}(x))$ in the CO gathers can be written as

$$q = \frac{d}{dx_m}T_{CO} = \frac{AT_0 + D(x_m - x_0)}{T_{CO}} \ , \quad (14)$$

Setting $x_m = x_0$ in equation 14, simplifies it to

$$AT_0 = q(x_0,t)T_{CO} \ , \quad (15)$$

which, in turn, can be used together with $t = T_{CO}$ to recast equation 14 in the form

$$D(x_m - x_0) = t[q(x_m,t) - q(x_0,t)] \ . \quad (16)$$

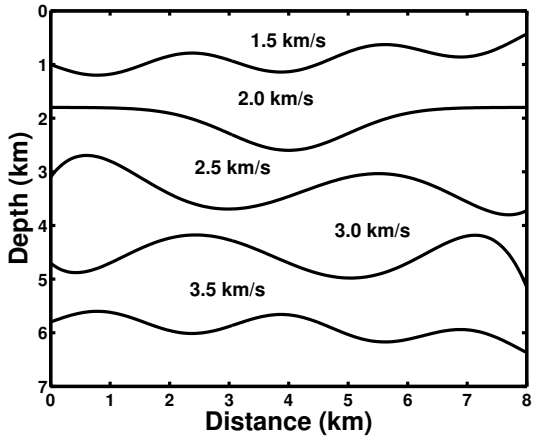

Figure 1: Synthetic model for the experiments.

Therefore, substituting the above expressions in Equation 12 and solving for the CMP traveltime, we obtain the coordinate map

$$t_{CMP} = \sqrt{t^2 - t(x_m - x_0)[q(x_m,t) + q(x_0,t)]}\ , \qquad (17)$$

between the CO and CMP sections. The coordinate map in Equation 17 can be executed once q has been detected at every point (x_m,t) in the CO section.

Combining the above equations, we can determine estimates a and b for parameters A and B in the CO section according to

$$a(x_0,t) = \frac{tq(x_0,t)}{t_0}\ , \qquad (18)$$

and

$$b(x_m,t) = \frac{t[q(x_m,t) - q(x_0,t)]}{x_m - x_0} - a(x_m,t)^2, \qquad (19)$$

with $x_m \neq x_0$. Note that the estimates $a(x_0,t)$ and $b(x_m,t)$ pertain to the single, chosen central point x_0. Therefore, they need to be transferred to the point (x_0,t_0) in the parameter sections.After changes of coordinates, as before for the case of the C section, many estimates of the parameters, A and B will be attributed to the same ZO time, t_0. Finally, the parameters A and B are calculated by average, just as it was done for parameter C.

Synthetic Example

Figure 1 shows the synthetic model of a stratified medium with four homogeneous layers bounded by smooth interfaces, between two half-planes, used in the numerical experiments. By means of ray tracing, the primary reflections of all interfaces were calculated together with the CRS parameters, A, B and C. Multi-coverage data acquisition was simulated with a total of 400 shots, recorded with 100 receivers in a common-shot configuration with 20% added noise. Shot-receiver intervals were 20m, resulting in 800 CMP locations. The seismic signal was a 30 Hz zero-phase Ricker wavelet and the sampling interval was 4 ms.

Three central points were chosen at $x_0 = 2.0$ km, $x_0 = 4.0$ km and $x_0 = 6.0$ km, and the values of parameters at these points, estimated by conventional CRS method. The values

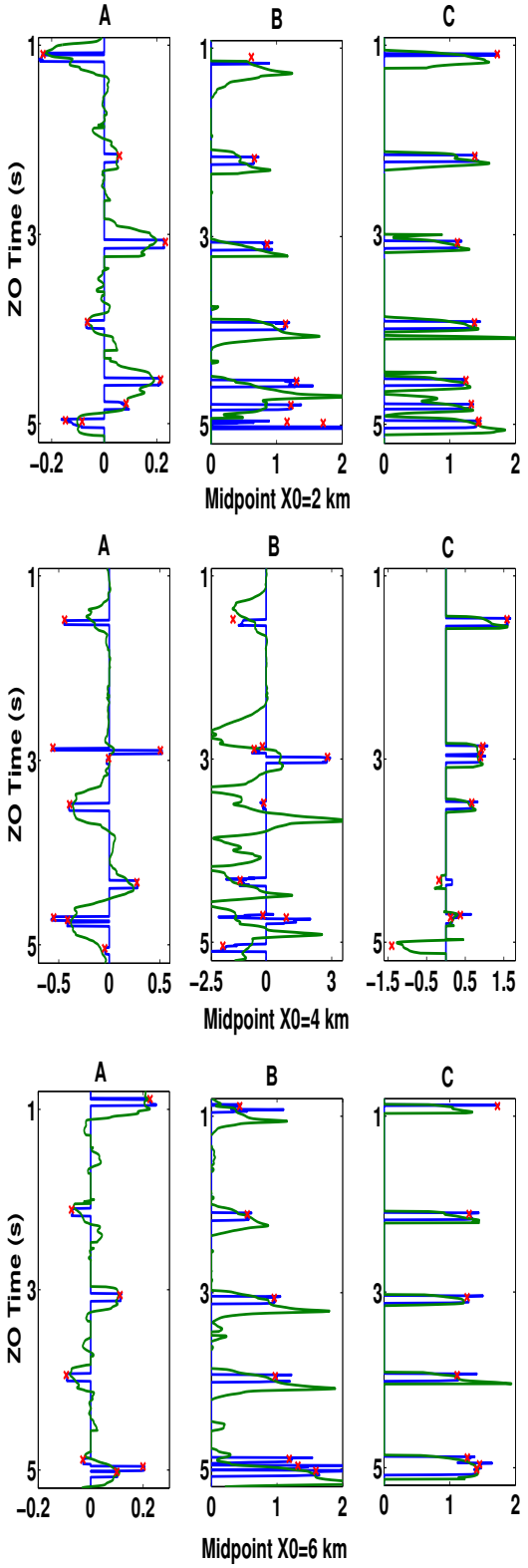

Figure 2: Experiments with 20% added noise. CRS parameters A, B and C at midpoints $x_0 = 2.0$ km (top), $x_0 = 4.0$ km (middle) and $x_0 = 6.0$ km (bottom), extracted by conventional CRS method (solid blue), local-slopes method (solid green) and their exact values (red crosses). Diferent semblance windows are used for eliminate spurious values on the CRS extracted parameters.

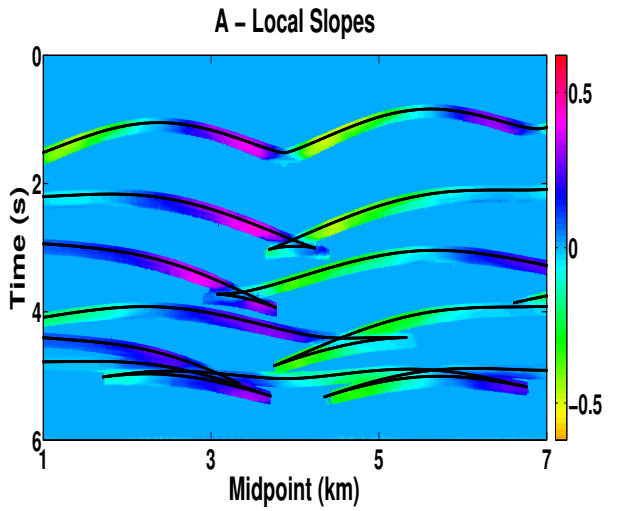

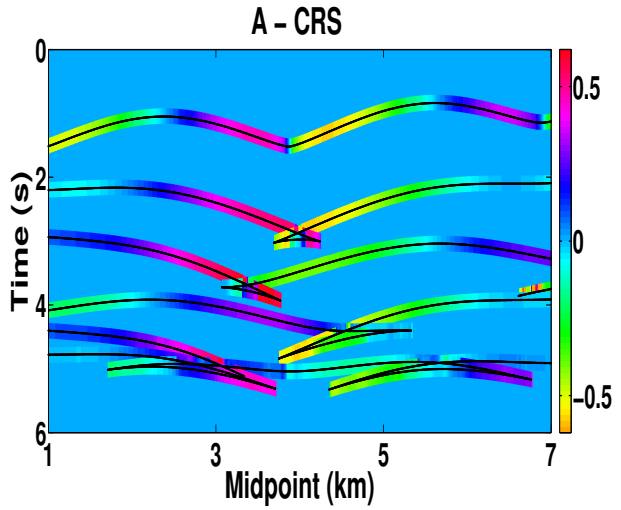

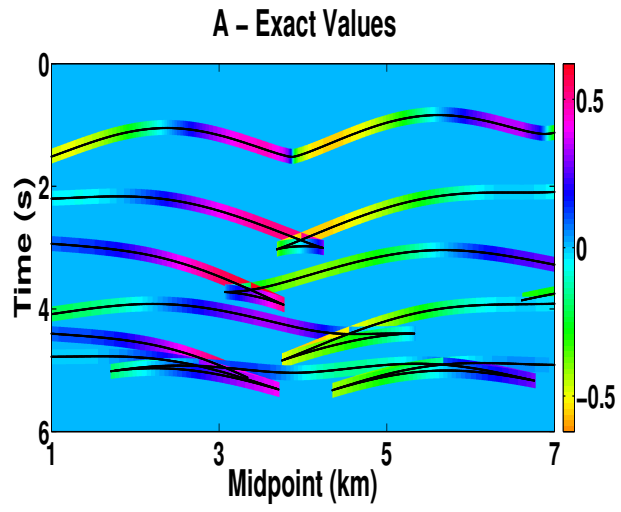

Figure 3: CRS parameter A for 600 central points between 1.0 km and 7.0 km for data with 20% noise added, as extracted by the local slopes method (top), by the conventional CRS method (middle) and the exact values calculated by means of ray tracing (bottom). A 0.6 semblance window is used for eliminate spurious values on the CRS extracted parameters.

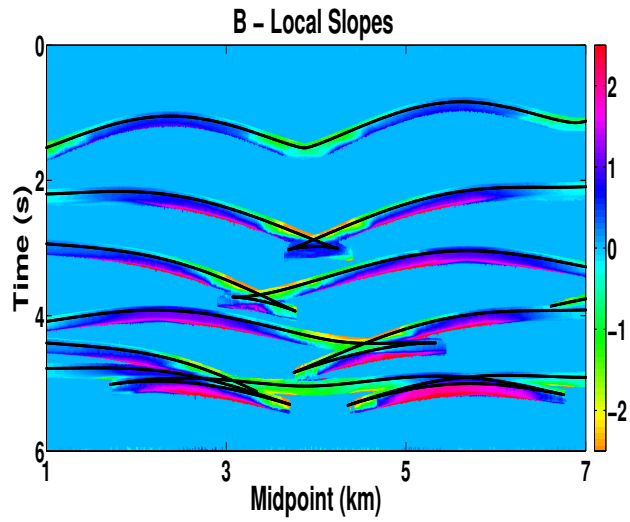

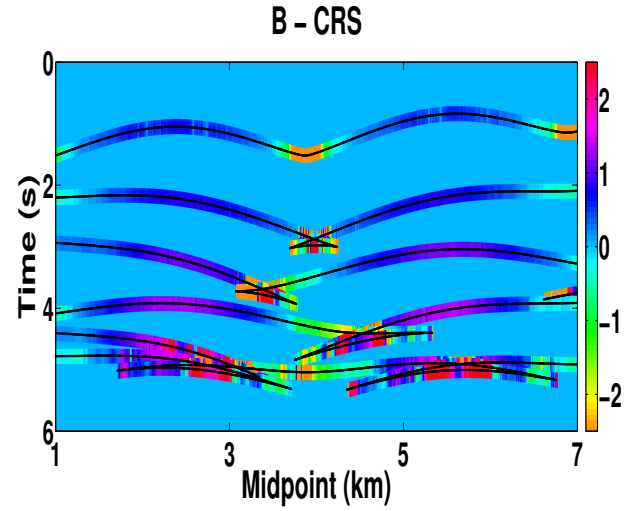

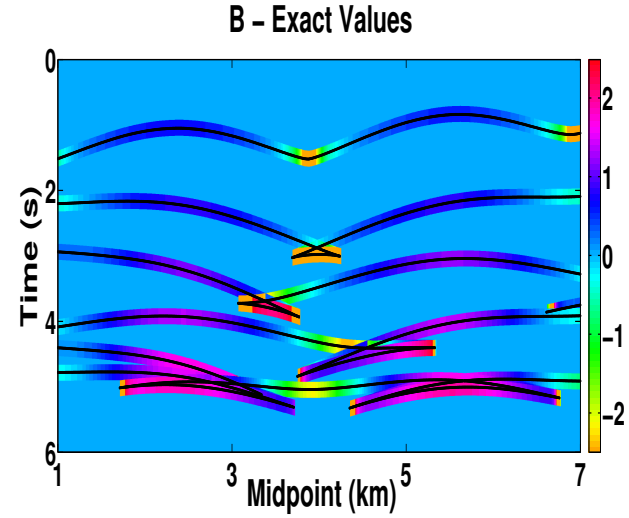

Figure 4: CRS parameter B for 600 central points between 1.0 km and 7.0 km for data with 20% noise added, as extracted by the local slopes method (top), by the conventional CRS method (middle) and the exact values calculated by means of ray tracing (bottom). A 0.6 semblance window is used for eliminate spurious values on the CRS extracted parameters.

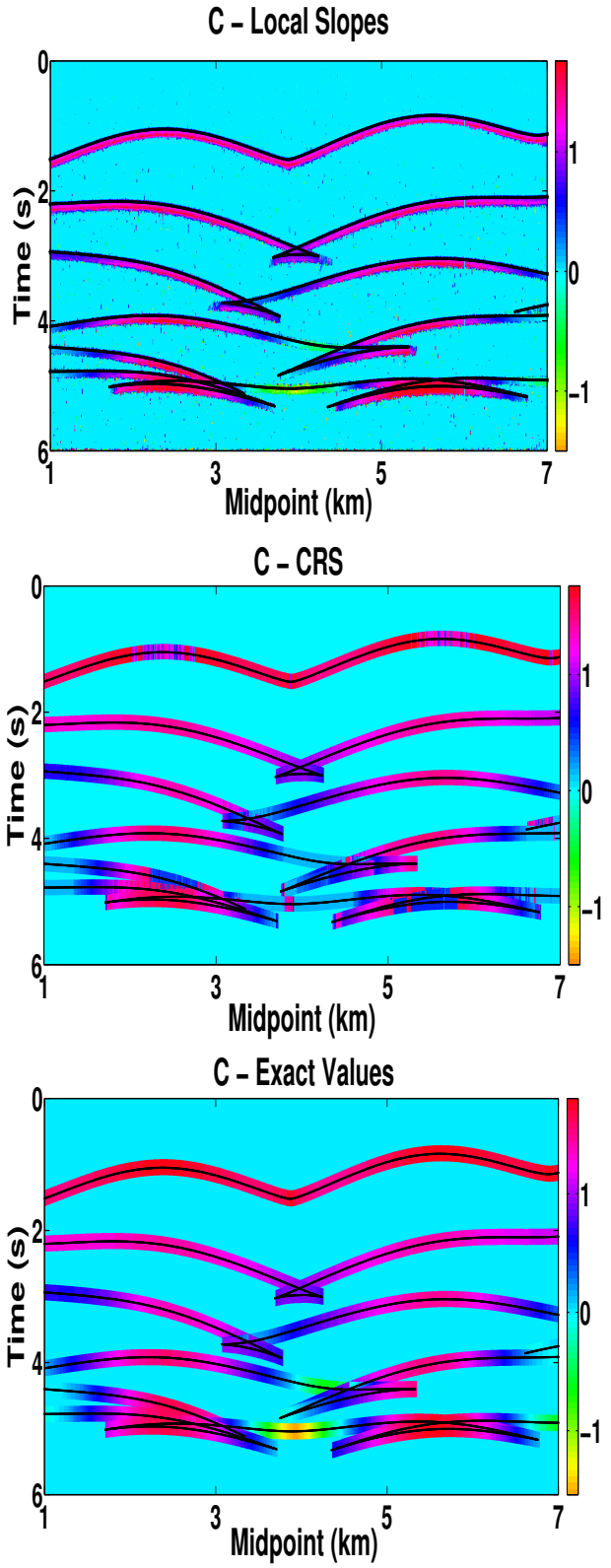

Figure 5: CRS parameter C for 600 central points between 1.0 km and 7.0 km for data with 20% noise added, as extracted by the local slopes method (top), by the conventional CRS method (middle) and the exact values calculated by means of ray tracing (bottom). A 0.6 semblance window is used for eliminate spurious values on the CRS extracted parameters.

of A, B and C parameters are depicted in Figure 2 (solid blue lines), together with the respective exact values (red crosses). Of course, exact values are only available at the reflection events, while the extraction procedure yields values at all times. Also in Figure 2 are depicted the values of the three parameters estimated by the local-slopes technique (solid green lines) at the same central points $x_0 = 2.0$ km, $x_0 = 4.0$ km and $x_0 = 6.0$ km. For this aim, we considered the CMP sections, taking the CMP location at these points, as well as only one CO section with half-offset 10m and 100 midpoints. Diferent semblance windows were used for eliminate spurious values on the local slopes extracted parameters.

Parameter sections

To compare the parameter extraction methods, we repeated the above experiments for 600 midpoints, between 1.0 km and 7.0 km, along the model of Figure 1. Figures 3, 4 and 5 show the parameter panels resulting from the local-slopes and conventional CRS methods applied to the 20% added noise data and the panels with the exact values, respectively. The panels are masked with the semblance section, muting all parameter values at points where the semblance value is below 0.6. Also shown in Figures 3, 4 and 5 are the times of the reflection events in the ZO section (black solid lines).

Conclusions

A new algorithm based on an automated extraction of local slopes in the data is able to estimate CRS parameters at a fraction of the cost of the conventional algorithm based on coherence analysis (semblance) procedures. Besides computational economy, first examples show that the slope extraction is sufficiently robust to allow for high-quality extraction of all CRS parameters from the extracted slope fields. The example also indicates that conventionally extracted CRS parameters are superior to those obtained from local slopes. This suggests using the slope-extracted parameters as initial values for a subsequent global search in the conventional CRS processing because it uses single-parameter optimizations in data subsets to determine these initial values. Such a procedure will imply a reduced overall processing time.

References

Castagna, J. P., and M. M. Backus, 1993, Offset-dependent reflectivity-theory and practice of avo analysis: Soc. of Expl. Geophys.

Claerbout, J. F., 1992, *in* Earth Sounding Analysis: Processing versus Inversion: Blackwell Scientific Publications.

Fomel, S., 2002, Aplications of plane-wave destruction filters: Geophysics, **67**, 1946–1960.

Hertweck, T., J. Schleicher, and J. Mann, 2007, Data stacking beyond CMP: The Leading Edge, **48**, 818–817.

Hubral, P., 1983, Computing true amplitude reflections in a laterally inhomogeneous earth: Geophysics, **48**, 1051–1062.

Hubral, P., G. Höcht, and R. Jäger, 1998, An introduction to the common reflection surface stack, *in* 60th Mtg.: Eur. Assn. Geosci. Eng., Session:1–19.

Neidel, N. S., and M. T. Taner, 1971, Semblance and other coherency measures for multichannel data: Geophysics, **36**, 482–497.

Ottolini, R., 1983, Velocity independent seismic imaging: SEP report, **37**, 59–67.

Santos, L. T., J. Schleicher, J. C. Costa, and A. Novais, 2011, Fast estimation of common-reflection-surface (CRS) parameters using local slopes: Geophysics, **76**, U23–U34.

Schleicher, J., J. C. Costa, L. T. Santos, A. Novais, and M. Tygel, 2009, On the estimation of local slopes: Geophysics, **74**, P25–P33.

Acknowledgments

This work was kindly supported by the Brazilian research agencies CAPES, FINEP and CNPq, as well as Petrobras, Brazil, and the sponsors of the *Wave Inversion Technology (WIT) Consortium*, Germany.